

Direct Measurement of Light Waves

E. Goulielmakis,^{1*} M. Uiberacker,^{1*} R. Kienberger,¹ A. Baltuska,¹ V. Yakovlev,¹ A. Scrinzi,¹ Th. Westerwalbesloh,² U. Kleineberg,² U. Heinzmann,² M. Drescher,² F. Krausz^{1,3†}

The electromagnetic field of visible light performs $\sim 10^{15}$ oscillations per second. Although many instruments are sensitive to the amplitude and frequency (or wavelength) of these oscillations, they cannot access the light field itself. We directly observed how the field built up and disappeared in a short, few-cycle pulse of visible laser light by probing the variation of the field strength with a 250-attosecond electron burst. Our apparatus allows complete characterization of few-cycle waves of visible, ultraviolet, and/or infrared light, thereby providing the possibility for controlled and reproducible synthesis of ultrabroadband light waveforms.

Although the wave nature of light has long been known, it has not been possible to measure directly the oscillating field of light. Radiation in the visible and higher frequency spectral ranges can so far only be characterized in terms of physical quantities averaged over the wave period. Nonlinear optical techniques now allow measurement of $\epsilon_L(t)$, the amplitude envelope, and $\omega_L(t)$, the carrier frequency, as a function of time t , for light pulses with durations that approach the wave cycle (1, 2). The carrier-envelope phase ϕ , which determines the timing between $\epsilon_L(t)$ and $\omega_L(t)$, can also be measured (3). These measurements rely on carrier-envelope decomposition, which is physically meaningful only as long as the frequency spectrum of the wave is confined to less than one octave (4). If the radiation is composed of frequencies spanning a broader range (5–17), direct access to the field is required. Attosecond pulses of extreme ultraviolet (XUV) light were predicted to suit for this purpose (18, 19). We report the direct measurement of the buildup and disappearance of the electric field of a light pulse through the use of an attosecond probe.

The electric field is defined as the force exerted on a point charge of unit value. Its conceptually most direct measurement must therefore rely on measurement of this force. In a light wave, the electric field E_L , and hence the force $F = qE_L$ it exerts on a particle with charge q , are subject to rapid variations. Access to this force is possible only if the probe charge is instantly placed in the field, i.e., within a time interval τ_{probe} over which

the temporal variation of the force is “frozen”, i.e., $\tau_{\text{probe}} \ll T_0 = (2\pi)/\omega_L$, where T_0 is the wave period. The probe charge can be launched into the field by knocking electrons free from atoms or ions instantly. In a linearly polarized wave, the change of the electrons' momentum $\Delta p(\vec{r}, t)$ at location \vec{r} and time t along the direction of the electric field is given by

$$\Delta p(\vec{r}, t) = e \int_{t'}^{\infty} E_L(\vec{r}, t') dt' = e A_L(\vec{r}, t) \quad (1)$$

where e is the electron charge and $A_L(\vec{r}, t)$ is the vector potential of the electric field $E_L(\vec{r}, t) = E_0 \epsilon_L(\vec{r}, t) \cos(kz - \omega_L t + \phi)$, where E_0 is the maximum field amplitude, and k is the wave vector. In our analysis, we assumed the wave to propagate along the z direction, and $t = t_{\text{real}} - z/v_g$ was defined in a retarded frame to yield $t = 0$ as locked to the peak of the pulse travelling at the group velocity v_g .

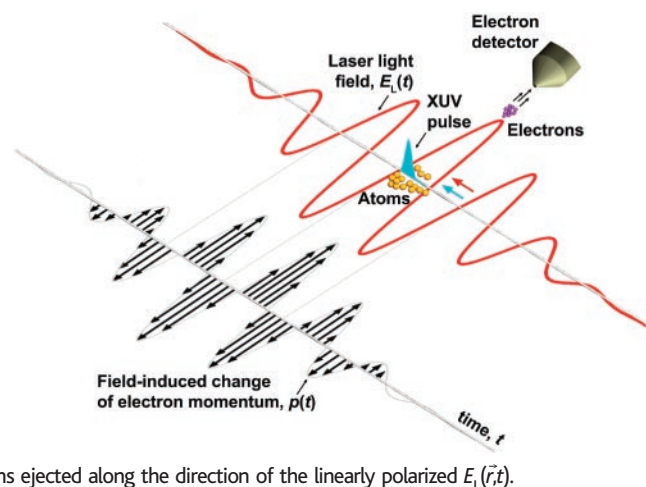
The relation $E_L(\vec{r}, t) = -\partial A_L(\vec{r}, t)/\partial t$ implies that measuring the momentum boost $\Delta p(\vec{r}, t)$ imparted to the freed electrons by the field at

the location \vec{r} at two instants differing in time by $\delta t \ll T_0/4$ will yield the electric field strength and direction directly as $E_L(\vec{r}, t) = [\Delta p(\vec{r}, t - \delta t/2) - \Delta p(\vec{r}, t + \delta t/2)]/e\delta t$. This measurement procedure relies on a momentary release of the electrons within $\tau_{\text{probe}} \leq T_0/4$. For near infrared, visible, and ultraviolet light, this condition dictates that $\tau_{\text{probe}} < 1$ fs. Varying the timing of such a subfemtosecond electron probe across the laser pulse provides complete information on the electric field of the light wave.

These considerations suggest that the electron probe needs to be localized not only in time to a tiny fraction of the wave period T_0 , but also in space to a tiny fraction of the wavelength λ_L of the light wave to be measured. The latter requirement can be substantially relaxed if we trigger the electron release with an energetic photon pulse that copropagates with the laser wave in a collinear beam (Fig. 1). Because the timing of the probe electrons relative to the light field is invariant to space in this case, in a gently focused laser beam they can be released and are subsequently allowed to move over distances substantially larger than λ_L , in a volume within which the spatial variation of the field amplitude $\epsilon_L(\vec{r}, t)$ is negligibly small for a fixed value of t .

Putting the above concept into practice requires the electron probe to be scanned through the entire laser pulse. For each newly set timing t , measurement of the momentum shift $\Delta p(t)$ of the probing electrons requires the laser pulse to pass through the measurement apparatus again. Full characterization of the light waveform is therefore only feasible if it can be reproducibly generated for repeated measurements. Another equally important prerequisite for implementation of the above concept is the availability of an energetic instantaneous excitation (for launching the probing electrons) that is not only confined temporally to a fraction of 1 fs but is also synchronized to the light wave with similar

Fig. 1. Schematic of the measurement principle. A few-cycle pulse of laser light, together with a synchronized subfemtosecond XUV burst, is focused into an atomic gas target. The XUV pulse knocks electrons free by photoionization. The light electric field $E_L(t)$ to be measured imparts a momentum change to the electrons (black arrows), which scales as the instantaneous value of the vector potential $A_L(t)$ at the instant of release of the probing electrons. The momentum change is measured by an electron detector, which collects the electrons ejected along the direction of the linearly polarized $E_L(\vec{r}, t)$.



¹Institut für Photonik, Technische Universität Wien, Gusshausstraße 27, A-1040 Wien, Austria. ²Fakultät für Physik, Universität Bielefeld, D-33615 Bielefeld, Germany. ³Max-Planck-Institut für Quantenoptik, Hans-Kopfermann-Strasse 1, D-85748 Garching, Germany.

*These authors contributed equally to this work.

†To whom correspondence should be addressed. E-mail: ferenc.krausz@tuwien.ac.at

accuracy. With the generation of waveform-controlled, intense, few-cycle light pulses (20) and their successful application to producing single 250-as XUV pulses synchronized to the driver light wave (21), these preconditions are now fulfilled. The waveform-controlled pulses—after having produced the attosecond photon probe—allow through nonlinear optical frequency conversion the synthesis of reproducible, synchronized, ultrabroadband, few-cycle waveforms (5–17). These can be repeatedly sent into the measurement apparatus with exactly the same waveform, and the subfemtosecond XUV pulse is able to produce the electrons by photoionization for probing the oscillating light field with sufficient temporal resolution.

The electrons knocked free from the atoms by the XUV pulse can be most conveniently detected if the direction of their movement is left unchanged by the light field. This applies if electrons are detected within a narrow cone aligned with the electric field vector of the linearly polarized laser wave along the x direction and are ejected with a large-enough initial momentum p_i to fulfill $|p_i| > |\Delta p_{\max}|$, where Δp_{\max} is the maximum momentum shift induced by the field. A large initial momentum also benefits the

measurement by enhancing the change of the electrons' kinetic energy ΔW , according to $\Delta W \approx (p_i/m)\Delta p$, and m is the electron's mass. This expression, together with Eq. 1, implies that the energy shift scales linearly with both the electric field and the wavelength of the light field to be probed (22). The importance of a large ΔW lies in the facts that the probing electrons are emitted with an inherent uncertainty $\delta W_{\text{probe}} \approx \hbar/\tau_{\text{probe}}$ (where \hbar is Planck's constant h divided by 2π) and that the dynamic range over which the light field strength can be reliably measured scales with $\Delta W_{\max}/\delta W_{\text{probe}}$ (ΔW_{\max} is the maximum shift in the pulse).

Measurement of $E_L(t)$ over a substantial dynamic range requires a ΔW_{\max} of several tens of electron volts. For an initial kinetic energy of $W_i \approx 100$ eV, this condition is satisfied for $E_0 < 10^8$ V/cm for near-infrared light and requires $E_0 \approx 3 \times 10^8$ V/cm for ultraviolet light (22). Noble gases with a low atomic number (such as helium and neon) safely resist ionization by a few-cycle field at these field strengths (23). The accuracy of definition of the location \vec{r} is dictated by the size of the volume within which $\epsilon(\vec{r}, t)$ is approximately independent of \vec{r} . If the field is

probed in the beam focus, this condition requires the probing electrons to be confined—laterally (xy) and longitudinally (z) to a small fraction of the diameter and to the confocal parameter of the beam, respectively.

In a proof-of-concept experiment, we directly measured the $E_L(t)$ of the few-cycle laser pulse used for producing the attosecond photon probe (Fig. 1). Linearly polarized, waveform-controlled, <5-fs, 0.4-mJ, 750-nm ($T_0 = 2.5$ fs) laser pulses (20), with carefully optimized values of ϕ and E_0 , produce single 250-as XUV pulses at $(\hbar\omega_{\text{xuv}})_{\text{mean}} = 93$ eV in a gas of neon atoms (21). The XUV pulse copropagates with the laser pulse in a collinear, laserlike beam to a second neon target placed in the focus of a spherical, two-component, Mo/Si multilayer mirror (21). The mirror, of 120-mm focal length, reflects XUV radiation over a band of ~ 9 eV, centered at ~ 93 eV. Consequently, the XUV pulse sets electrons free by photoionization with an initial kinetic energy of $p_i^2/2m = \hbar\omega_{\text{xuv}} - W_b$, (where W_b is the electron's binding energy) spread over an ~ 9 -eV band, implying that $\delta W_{\text{probe}} \approx 9$ eV. The electrons' energy shift $\Delta W(t) \approx e(p_i/m)A_L(t)$ probes the laser vector potential. The volume of light-field probing is defined laterally by the <10 - μm diameter of the XUV beam at its waist and longitudinally by the <50 - μm size of the neon jet, which is well confined within the focal volume of the laser beam (diameter, >60 μm ; confocal parameter, >5 mm). For $p_i^2/2m \approx 100$ eV, the electrons traveled less than 1 μm within 100 fs and hence remained safely confined to the region of constant laser field amplitude.

The field-induced variation of the final energy spectrum of the probe electrons versus delay between the XUV burst and the laser pulse (Fig. 2) reveal, without the need of any detailed analysis, that probing is implemented by a single burst of subfemtosecond duration that is synchronized with subfemtosecond accuracy to the measured laser field. $E_L(t)$ can now be directly (i.e., without any iterative steps) obtained through the procedure outlined above (Fig. 3). From the measured spectrum of the few-cycle laser pulse (Fig. 3, inset), we calculated $E_L(t)$ by a simple Fourier transformation on the assumption of absence of spectral phase variations. The result, with E_0 and ϕ chosen to yield the best match to the measured values, is shown in gray. The excellent fit to the measured field evolution indicates a near-transform-limited pulse. Its duration was evaluated as 4.3 fs, in good agreement with the result of an autocorrelation measurement.

It has been predicted by theory that the few-cycle pulse pumping the XUV source has a "cosine" waveform ($\phi \approx 0$) if a single subfemtosecond pulse emerges from the ionizing atoms (24). Our results (Fig. 3) yield the exper-

Fig. 2. A series of kinetic energy spectra of electrons detached by a 250-as, 93-eV XUV pulse from neon atoms in the presence of an intense <5-fs, 750-nm laser field, in false-color representation. The delay of the XUV probe was varied in steps of 200 as, and each spectrum was accumulated over 100 s. The detected electrons were ejected along the laser electric field vector with a mean initial kinetic energy of $p_i^2/2m \approx \hbar\omega_{\text{xuv}} - W_b = 93$ eV $- 21.5$ eV $= 71.5$ eV. The energy shift of the electrons versus the timing of the XUV trigger pulse that launches the probing electrons directly represents $A_L(t)$. arb. u., arbitrary units.

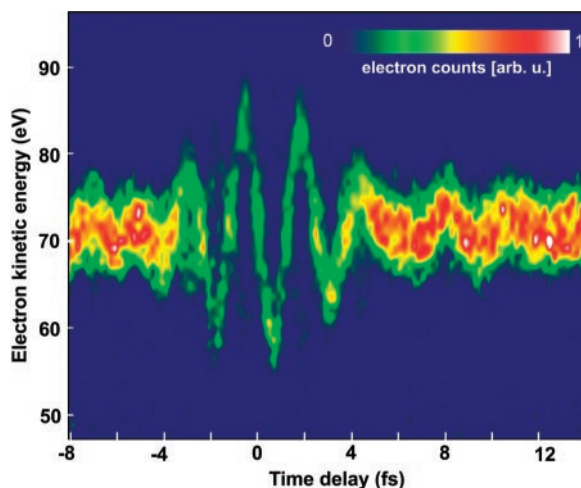
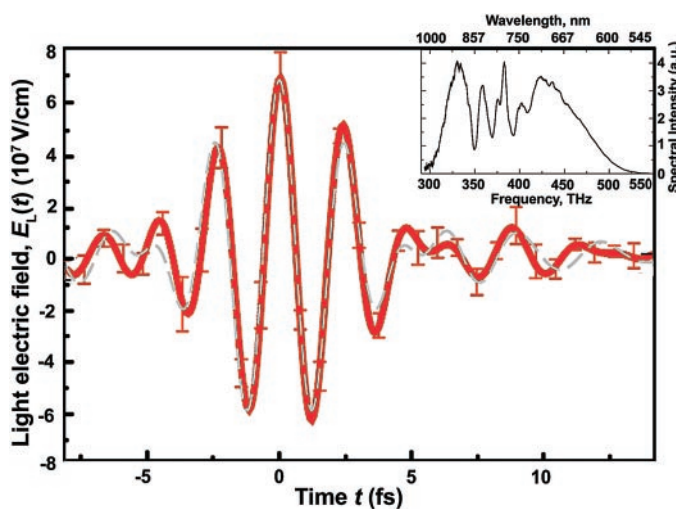


Fig. 3. $E_L(t)$ reconstructed (red line) from the data depicted in Fig. 2 and calculated (gray line) from the measured pulse spectrum (inset) with the assumed absence of a frequency-dependent phase and with E_0 and ϕ chosen so as to afford optimum matching to the measured field evolution. a.u., arbitrary units.



imental evidence. From this measurement, we also learn that the electric field points toward the electron detector at the pulse peak and that its strength is $\sim 7 \times 10^7$ V/cm. With the temporal evolution, strength, and direction of $E_{\perp}(t)$ measured, we have performed a complete characterization of a light pulse in terms of its classical electric field.

Direct probing of light-field oscillations represents what we believe to be a substantial extension of the basic repertoire of modern experimental science. The door to practical applications is opened by the creation of the key element of the demonstrated light-field detector, the synchronized attosecond electron probe, in a noninvasive manner. In fact, our intense <5 -fs laser pulse appears to be capable of producing the necessary XUV trigger burst without suffering any noticeable back-action to its own temporal shape (Fig. 3). After having produced the attosecond photon probe, this powerful few-femtosecond pulse is ideally suited for the synthesis of ultrabroadband, few-cycle, optical waveforms (5–17). Being composed of radiation extending from the infrared through the visible to the ultraviolet region, the resultant few-cycle, monocycle, and conceivably even subcycle waveforms will offer a marked degree of control over the temporal variation of electric and magnetic forces on molecular and atomic time scales.

These light forces, in turn, afford the promise of controlling quantum transitions of electrons in atoms and molecules and—at relativistic intensities—their center-of-mass motion. Reproducible ultrabroadband light wave synthesis, a prerequisite for these prospects to materialize, is inconceivable without subfemtosecond measurement of the synthesized waveforms. Beyond providing the subfemtosecond electron probe for these measurements, the substantial experimental efforts associated with the construction and reliable operation of a subfemtosecond photon source will pay off in yet another way. The envisioned control of electronic motion with light forces can only be regarded as accomplished once it has been measured. Owing to their perfect synchronism with the synthesized light waveforms, the subfemtosecond photon probe will allow us to test the degree of control achieved by tracking the triggered (and hopefully steered) motion in a time-resolved fashion.

References and Notes

1. R. Trebino *et al.*, *Rev. Sci. Instrum.* **68**, 3277 (1997).
2. C. Iaconis, I. A. Walmsley, *Opt. Lett.* **23**, 792 (1998).
3. G. G. Paulus *et al.*, *Phys. Rev. Lett.* **91**, 253004 (2003).
4. T. Brabec, F. Krausz, *Phys. Rev. Lett.* **78**, 3282 (1997).
5. T. W. Hänsch, *Opt. Commun.* **80**, 71 (1990).
6. S. Yoshikawa, T. Imasaka, *Opt. Commun.* **96**, 94 (1993).
7. A. E. Kaplan, P. L. Shkolnikov, *Phys. Rev. Lett.* **73**, 1243 (1994).
8. K. Shimoda, *Jpn. J. Appl. Phys.* **34**, 3566 (1995).
9. S. E. Harris, A. V. Sokolov, *Phys. Rev. Lett.* **81**, 2894 (1998).
10. A. Nazarkin, G. Korn, *Phys. Rev. Lett.* **83**, 4748 (1999).
11. O. Albert, G. Mourou, *Appl. Phys. B* **69**, 207 (1999).

12. M. Wittman, A. Nazarkin, G. Korn, *Phys. Rev. Lett.* **84**, 5508 (2000).
13. Y. Kobayashi, K. Torizuka, *Opt. Lett.* **25**, 856 (2000).
14. A. V. Sokolov, D. R. Walker, D. D. Yavuz, G. Y. Yin, S. E. Harris, *Phys. Rev. Lett.* **87**, 033402 (2001).
15. K. Yamane *et al.*, *Opt. Lett.* **28**, 2258 (2003).
16. M. Y. Shverdin, D. R. Walker, D. D. Yavuz, G. Y. Yin, S. E. Harris, in *OSA Trends in Optics and Photonics Series (TOPS) Vol. 96, Conference on Lasers and Electro-Optics (CLEO)* (Optical Society of America, Washington, DC, 2004), Postdeadline paper CPDC1.
17. K. Yamane, T. Kito, R. Morita, M. Yamashita, in *OSA Trends in Optics and Photonics Series (TOPS)*, vol. 96, *Conference on Lasers and Electro-Optics (CLEO)*, (Optical Society of America, Washington, DC, 2004), Postdeadline paper CPDC2.
18. R. Kienberger *et al.*, *Science* **297**, 1144 (2002).
19. A. D. Bandrauk, Sz. Chelkowski, N. H. Shon, *Phys. Rev. Lett.* **89**, 283903 (2002).
20. A. Baltuska *et al.*, *Nature* **421**, 611 (2003).
21. R. Kienberger *et al.*, *Nature* **427**, 817 (2004).
22. In the limit of $|\Delta p_{\max}| \ll |p_i|$, the change in the electrons' final kinetic energy is given by $\Delta W_{\max} \approx [8W/U_{p,\max}]^{1/2}$, where $U_{p,\max} = e^2 E_0^2 / 4m_e \omega_L^2$ is the electrons' quiver energy averaged over an optical cycle at the peak of the light pulse.
23. Increase of the excitation energy $\hbar\omega_{\text{XUV}}$ tends to reconcile the conflicting requirements of avoiding field ionization and ensuring a high dynamic range.
24. T. Brabec, F. Krausz, *Rev. Mod. Phys.* **72**, 545 (2000).
25. We are grateful to B. Ferus for creating the artwork. Sponsored by the fonds zur Förderung der Wissenschaftlichen Forschung (Austria, grant nos. Y44-PHY, P15382, and F016), the Deutsche Forschungsgemeinschaft and the Volkswagenstiftung (Germany), the European ATTO and Ultrashort XUV Pulses for Time-Resolved and Non-Linear Applications networks, and an Austrian Programme for Advanced Research and Technology fellowship to R.K. from the Austrian Academy of Sciences.

28 May 2004; accepted 20 July 2004

Nanoribbon Waveguides for Subwavelength Photonics Integration

Matt Law,^{1,2*} Donald J. Sirbuly,^{1,2*} Justin C. Johnson,¹ Josh Goldberger,¹ Richard J. Saykally,¹ Peidong Yang^{1,2†}

Although the electrical integration of chemically synthesized waveguides has been achieved with lithography, optical integration, which promises high speeds and greater device versatility, remains unexplored. We describe the properties and functions of individual crystalline oxide nanoribbons that act as subwavelength optical waveguides and assess their applicability as nanoscale photonic elements. The length, flexibility, and strength of these structures enable their manipulation on surfaces, including the optical linking of nanoribbon waveguides and other nanowire elements to form networks and device components. We demonstrate the assembly of ribbon waveguides with nanowire light sources and detectors as a first step toward building nanowire photonic circuitry.

Photonics, the optical analog of electronics, shares the logic of miniaturization that drives research in semiconductor and information technology. The ability to manipulate pulses of light within sub-micrometer volumes is vital for highly integrated light-based devices, such as optical computers, to be realized. Recent advances in the use of photonic band gap (1, 2) and plasmonic (3, 4) phenomena to control the flow of light are impressive in this regard. One alternative route to integrated photonics is to assemble photonic circuits from a collection of nanowire elements that assume different functions, such as light creation, routing, and detection. Chemically synthesized nanowires have several features that make them good photonic building blocks, including inherent one-dimensionality, a di-

versity of optical and electrical properties, good size control, low surface roughness, and, in principle, the ability to operate above and below the diffraction limit. The toolbox of nanowire device elements already includes various types of transistors (5), light-emitting diodes (6), lasers (7, 8), and photodetectors (9). An important step toward nanowire photonics is to develop a nanowire waveguide that can link these various elements and provide the flexibility in interconnection patterns that is needed to carry out complex tasks such as logic operations (10). Our demonstration of nanowire-based photonics complements and expands upon recent work on optical beam steering in mesostructured silica cavities (11) and on subwavelength structures made lithographically (12, 13) and by the drawing of silica microfibers (14).

Nanoscale ribbon-shaped crystals of binary oxides exhibit a range of interesting properties including extreme mechanical flexibility, surface-mediated electrical conductivity (15), and lasing (16). As part of a recent study of the photoluminescence (PL) of SnO₂ nanoribbons, we noted that ribbons with high

¹Department of Chemistry, University of California, Berkeley, CA 94720, USA. ²Materials Science Division, Lawrence Berkeley National Laboratory, 1 Cyclotron Road, Berkeley, CA 94720, USA.

*These authors contributed equally to this work.

†To whom correspondence should be addressed. E-mail: p_yang@uclink.berkeley.edu